

Acceleration of the Solar Wind by Ambipolar Electric Field

Viviane Pierrard^{1, 2, a)} and Maximilien Péters de Bonhome^{1, 2, b)}

¹*Solar-Terrestrial Center of Excellence and Space Physics, Royal Belgian Institute for Space Aeronomy, B-1180 Brussels, Belgium .*

²*Center for Space Radiations, ELIC, Université Catholique de Louvain, B-1348 Louvain-La-Neuve, Belgium*

^{a)}Corresponding author: viviane.pierrard@aeronomie.be

^{b)}maximilien.peters@student.uclouvain.be

Abstract. Kinetic exospheric models revealed that the solar wind is accelerated by an ambipolar electric field up to supersonic velocities. The presence of suprathermal Strahl electrons at the exobase can further increase the velocity to higher values, leading to profiles comparable to the observations in the fast and slow wind at all radial distances. Such suprathermal electrons are observed at large distances and recently at low distances as well. Those suprathermal electrons were introduced into the kinetic exospheric model using Kappa distributions. Here, the importance of the exobase's altitude is also underlined for its ability to maintain the electric potential to a higher level for slower winds, conversely to what is induced through the effect of a lower kappa index only. In fact, the exobase is located at lower altitude in the coronal holes where the density is smaller than in the other regions of the corona, allowing the wind originating from the holes to be accelerated from lower distances to higher velocities.

The new observations of Parker Solar Probe (PSP) and Solar Orbiter (SolO) from launch to mid-2023 are here used to determine the characteristics of the plasma in the corona so that the model fits best to the averaged observed profiles for the slow and fast winds. The observations at low radial distances show suprathermal electrons already well present in the Strahl in the antisunward direction and a deficit in the sunward direction, confirming the exospheric feature of almost no incoming particles.

INTRODUCTION

The physical mechanisms responsible for the heating of the corona and the acceleration of the solar wind remain a hot topic of research ([1, 2] for reviews). Exospheric models provide a very simplified first approximation: considering only the effects of the external force, they show that the electric potential can accelerate the wind to supersonic velocities, even considering simple Maxwellian distributions for the particles at the exobase [3]. Moreover, the possible presence of suprathermal particles in the corona has important effects on the plasma temperature increase, and an enhanced population of energetic electrons accelerates the solar wind to larger bulk velocities, especially in case of a low exobase [4, 5, 6]. This gives a natural explanation for the fast wind originating from coronal holes, where the density is lower than in the other coronal regions. Differential heating and acceleration of minor ions can also be predicted using the exospheric approach, in agreement with ion observations in the solar wind [7]. Exospheric models predict too high temperature anisotropies (T_{\parallel}/T_{\perp}) in comparison to observations, which could be corrected by including effects of Coulomb collisions [8]. Waves like whistlers can also transform the velocity distributions and lead to more realistic heat fluxes [9, 10]. Plasma turbulence and instabilities modify the characteristics of the observed distributions, and especially their temperature anisotropies and heat fluxes [11].

In his groundbreaking work on the first predictive thermally-driven solar wind model, Parker [12] utilized magnetohydrodynamic (MHD) approach to successfully predict high velocities even before any measurements were possible in space. The MHD approach was later complemented by the kinetic exospheric approach showing the importance of the ambipolar electric field to accelerate the wind. Other solar wind acceleration processes have been proposed, involving magnetic reconnection and waves. Some of these effects can be included in the model via the boundary conditions and diffusion coefficients in the Fokker-Planck equation [8, 13].

The NASA mission Parker Solar Probe (PSP) makes unprecedented measurements at very low distances from the Sun, allowing to discover new features such as broadband electrostatic waves in the near-Sun solar wind [14]. It also provides the unique opportunity to study the radial evolution of the solar wind in the inner heliosphere by comparing observations with predictions from different models. A deficit in the sunward direction is observed in the PSP electron distributions at low radial distances, confirming the exospheric feature [15]. The deficit occurs in 60% – 80% of electron observations within 0.2 AU, and even more frequently in plasma with low collisional age, and a more anisotropic electron core population. The cutoff energy varies linearly with the local electron core temperature, confirming a direct relationship to the electric potential [16]. PSP also provides information on the presence of suprathermal electrons at very low distance [17] and the formation of the strahl and halo [18, 19].

In the present work, we constrain the exospheric Kappa model presented in Section 2 to provide the best fits with the profiles of the averaged moments observed by PSP, Solar Orbiter and OMNI shown in Section 3. The correlation

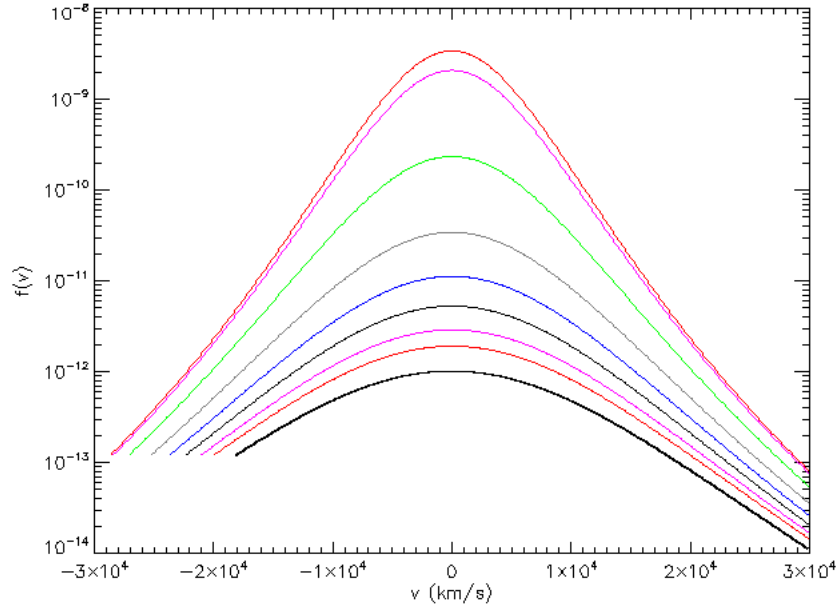


FIGURE 1. The electron velocity distribution function in the exospheric model for $\kappa=4$ at different radial distances starting from the exobase at 1.17 Rs (top in red) to 1.2 Rs (pink), 1.5 (green), 2 (grey), 2.5 (blue), 3 (dark grey), 3.5 (purple), 4 (red), and 5 Rs (bottom in black).

between proton temperatures and velocity will be discussed in section 4 in the framework of the possibility it gives to discriminate slow and fast winds. Electric field and heat flux obtained with the model constrained by the observations will be illustrated and discussed in section 5. Concluding remarks will be presented in the last section.

EXOSPHERIC MODEL

The Lorentzian exospheric model has been developed assuming a Kappa distribution for the electrons in ion exospheres [4, 20, 21]. The solar wind exospheric model has been recently improved by considering regularized Kappa distributions [22, 23] that have no diverging moments through consideration of a cut-off at relativistic velocities. The model becomes valid even for kappa indices lower than 2, which was needed since low values of kappa are sometimes observed in the fast solar wind [19].

Assuming velocity distribution functions of the particles at the exobase, we can determine the distributions at all radial distances, and thus calculate their different moments [24]. The presence of enhanced suprathermal electron tails accelerates the wind above the exobase in exospheric regions by increasing the electric potential and the flux of escaping electrons.

In the present exospheric model, the distribution is a regularized Kappa function truncated for negative velocities lower than minus the escape velocities [4, 25]. Indeed, if the electrons escape, they don't come back to the Sun which leads to an empty region of velocity space, i.e., a deficit of particles in the sunward direction. The escape velocity decreases with the radial distance and the suprathermal tails decrease less with the distance than the core, due to the velocity filtration effect [26, 27]. This is well visible on Figure 1 showing the electron truncated Kappa distribution from 1.7 Rs (upper red line) to 5.0 Rs (lower black line), with intermediate distances at 1.2 Rs, 1.5, 2, 2.5, 3, 3.5, and 4.

The most recent observations of PSP confirm such a deficit in the electron distributions at low distances [15]. They also show the existence of suprathermal electrons even at very low radial distances [17, 28], which was already observed with Helios for distances higher than 0.35 AU [13, 29]. The quantity of suprathermal electrons is even higher at large distances (> 1 AU) as indicated by lower values of the kappa index [30, 31, 32].

ANALYSIS OF RECENT SOLAR WIND OBSERVATIONS TO CONSTRAIN THE MODEL

In the present work, we analyze recent data from different spacecraft:

- Parker Solar Probe (PSP) from the 24th of January 2020 to the 30th of March 2023 from 13 to 50 R_s ,
- Solar Orbiter (SolO) from the 7th of July 2020 to the 30th of May 2023 from 63 to 218 R_s ,
- OMNI from the 7th of July 2020 to the 30th of May 2023 at 215 R_s (1 AU).

The observations from SolO and OMNI are discriminated using wind velocity $u < 400$ km/s for the slow wind and $u > 500$ km/s for the fast wind.

The criteria chosen for the selection of the fast and slow solar wind case of course influence the averaged values of the moments. The averaged velocity in the fast wind is slightly lower than in [19] since $u > 600$ km/s was chosen for the fast wind selection. Moreover, the recent observations of PSP and SolO contain much more fast solar wind cases than in [19] since the available data were limited to March 2022. Indeed, the solar activity is in its increasing phase with the next maximum expected in 2025.

For PSP, the criteria have to be different than SolO and OMNI because the observations are located in the acceleration region close to the Sun. This implies that distinguishing fast and slow winds using solely a velocity criterion is not sufficient since a considerable acceleration remains until the wind reaches its final velocity. Halekas et al. (2022) [33] assessed the remaining acceleration by computing the asymptotic speed which requires a measure of the electric potential at each wind velocity measurements. To avoid the need of this electric potential, an indirect way of estimating the remaining acceleration based on the correlation between the wind velocity and the proton temperature is proposed here and will be discussed in the next section.

In Figures 2, 3, and 4, the points represent the average values of the data (respectively the bulk velocity, density and proton temperature), and the colored area represents the double of the standard deviation interval around average value. This was obtained by binning data for each 4 R_s interval for PSP and 8 R_s for SolO and OMNI starting from the lowest registered distance of the corresponding set of data. The average and standard deviation was then computed on each of those bins [34]. Note that the gap between the observations of PSP and SolO is due to the lack of sufficiently accurate measurements beyond 50 R_s from PSP.

These figures also show a comparison with the profiles obtained with the exospheric Kappa model where the parameters of the model have been chosen in order to best fit the averaged observed values of Parker Solar Probe (PSP) Solar Orbiter (SolO) and OMNI at 1 AU, respectively in orange for the fast solar wind (FSW) and blue for the slow solar wind (SSW). The parameters found for the exospheric model are provided in Table 1.

Figure 2 illustrates the model capabilities of producing a realistic bulk velocity by setting the parameters found in Table 1 constrained by PSP, SolO, and OMNI averaged data separated in fast and slow wind. The main parameters that are responsible for the acceleration of the solar wind are the exobase level and the kappa index. In fact, a lower exobase and/or a lower kappa index will accelerate the wind. Furthermore, any changes in the exobase's altitude is much more effective when kappa is small. It is worth noting that when the fast wind is considered above 500 km/s, the corresponding kappa index is 2.4 (see Table 1), while it was estimated as 2.23 when the fast wind was considered above 600 km/s in [19].

Figure 3 shows the density profiles of the observations and the model. As expected, the density decreases faster in the fast wind than in the slow wind. The density at the exobase is the main parameter that needs to be constrained in the model to best reproduce the observations. Note that the SPAN-I instruments of PSP are not well calibrated to measure low densities [35], which could explain the apparent discontinuity between PSP and SolO observations that can not be resolved by extrapolating the trend.

TABLE 1. This table gives the parameters used in the exospheric model to best reproduce the Slow (SSW) and Fast Solar Wind (FSW) as observed on average by PSP, SolO, and OMNI up to 1 AU.

Wind type Symbol [units]	Exobase r_0 [R_s]	Exobase density $n(r_0)$ [m^{-3}]	Electron temperature $T_e(r_0)$ [K]	Proton temperature $T_p(r_0)$ [K]	kappa electrons κ
SSW	3.9	1.2×10^{11}	1.5×10^6	1.25×10^6	5
FSW	1.25	1.4×10^{12}	1.35×10^6	4.06×10^6	2.4

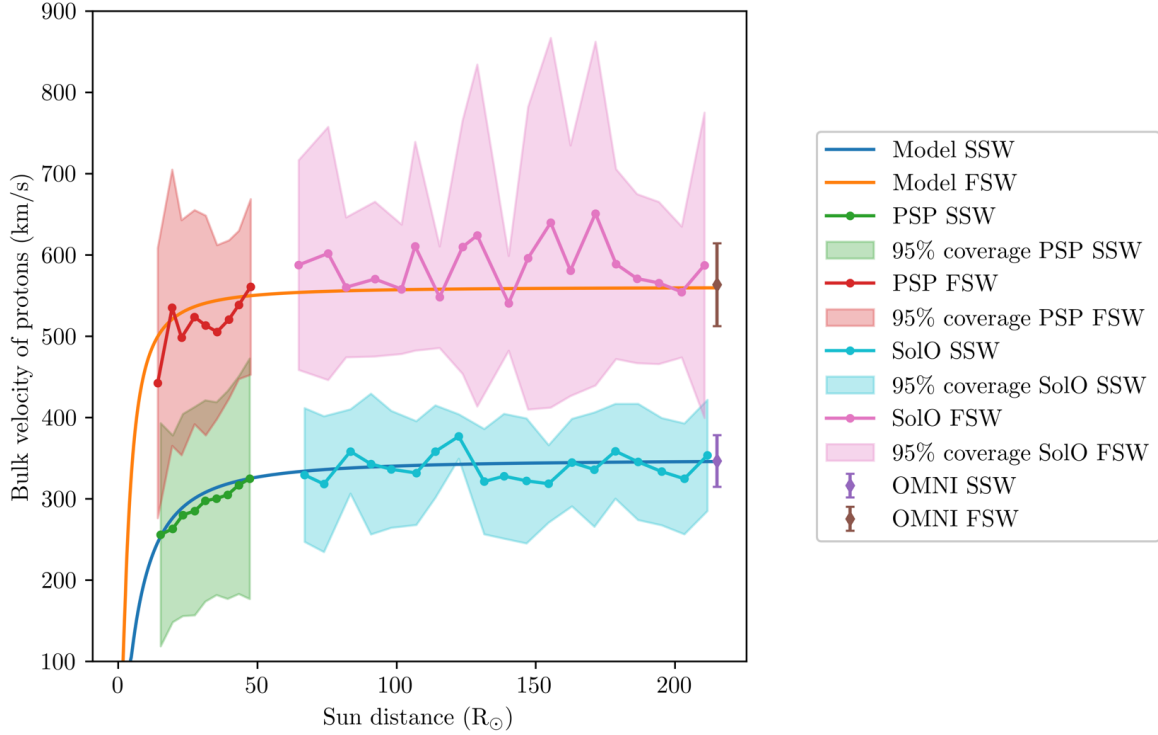


FIGURE 2. Averaged bulk velocity of protons and electrons as a function of the solar distance for the exospheric model constrained by averaged observations of Parker Solar Probe ($< 50 R_s$), Solar Orbiter ($> 63 R_s$), and OMNI ($215 R_s$) for fast solar wind (FSW in orange) and slow solar wind (SSW in blue).

Figure 4 shows the proton temperature profiles of the observations and the model. The temperature $T_p(r_0)$ at the exobase can be adjusted in the model to best reproduce the observations in the corona. One can see that the temperatures at 1 AU approximately correspond to the observations of OMNI (that are slightly lower than the averaged observations obtained by SolO at this same distance, probably due to the fact that SolO and OMNI does not always observe the same kind of events from their respective locations on the ecliptic plane). Both temperatures decrease too fast in comparison to the observations of SolO and PSP. This is due to the strong assumption of absence of interactions in the exospheric model. It is worth noting that extrapolating the trend of PSP measurements would not resolve the discontinuity with SolO measurements. This is due to the exceptional events that PSP has encountered during its close approaches coupled with the fact that the criteria distinguishing fast and slow wind is not only based on the velocity for PSP data (while it is for SolO data) but is rather a combination between velocity and temperature that will be discussed in the next section.

THE TEMPERATURE-VELOCITY CORRELATION USED AS SOURCE OF IDENTIFICATION

As obtained in [13] at 1 AU with Helios and CLUSTER and confirmed at lower distances with PSP observations [36], there is a strong correlation between the proton temperature and the velocity. This correlation is illustrated in Figure 5 between 48-50 Rs using PSP data. One finds a linear regression (blue line) with a correlation coefficient of 90 %.

Two Solar Energetic Particle events have been noticed in PSP data, one in early September 2022 and one in mid-March 2023. These events are characterized by higher temperatures than expected, thus deviating from the direct correlation that has been established during multiple other orbits at all distances in PSP data. The data points corresponding to those events have not been considered in Figure 5 and in aforementioned figures.

The observed correlation (illustrated by the linear regression in blue line) can be used to identify slow and fast wind

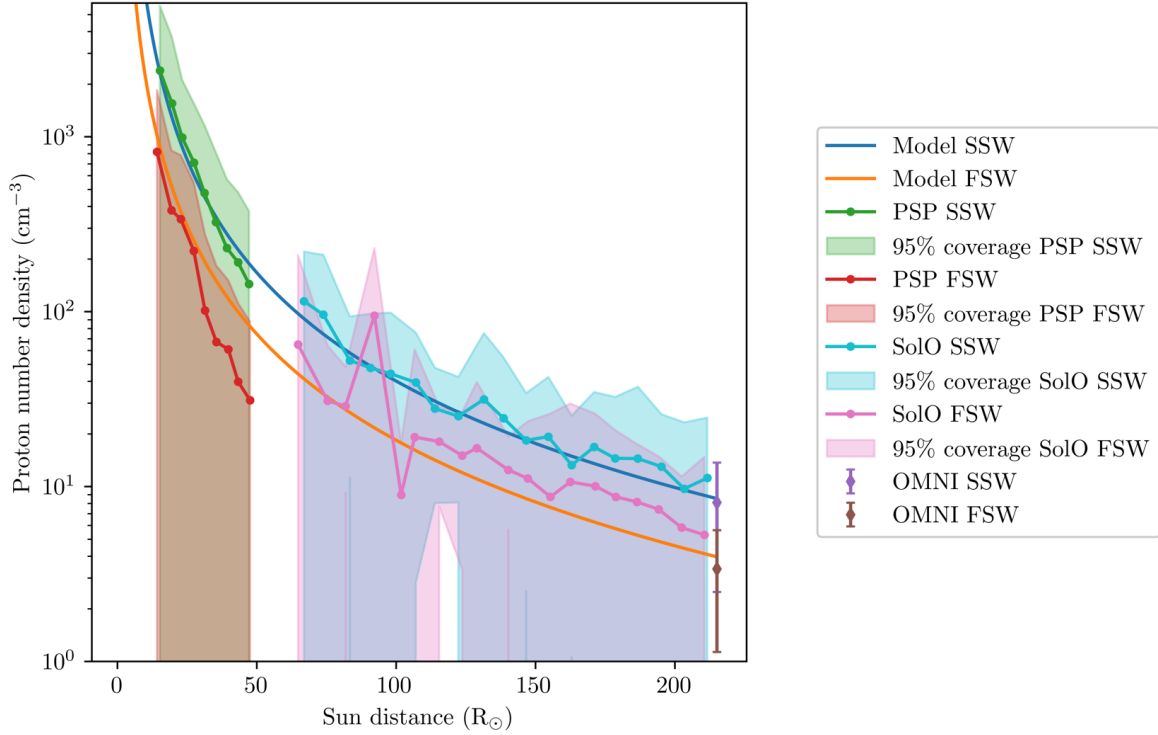


FIGURE 3. Averaged number density of protons and electrons as a function of the solar distance for the exospheric model constrained by averaged observations of Parker Solar Probe ($< 50 R_{\odot}$), Solar Orbiter ($> 63 R_{\odot}$), and OMNI ($215 R_{\odot}$) for fast solar wind (FSW in orange) and slow solar wind (SSW in blue).

at low radial distances where the final velocity is not yet reached. In the case of low radial distance, we define the slow solar wind observed by PSP as the points located below the orange line in Figure 5. This line is perpendicular to the linear regression (blue line) and intersects it at 450 km/s. The fast wind correspond to the points above the green perpendicular line crossing the regression at 500 km/s. The points between the two lines are excluded to better discriminate slow and fast winds. This gives better results than just separating the velocities below 450 km/s and above 500 km/s at low distances. It is here assumed that most of the winds with sufficiently high proton temperature (and velocity) will have a significant remaining acceleration, allowing them to be considered as fast solar winds where they would sometimes have been considered slow if a simple velocity criterion was considered.

ELECTRIC FIELD IN HYDRODYNAMIC AND EXOSPHERIC MODELS

Parker [1958] [12] was the first one to propose an hydrodynamic model for the solar atmosphere, giving up the hypothesis of hydrostatic equilibrium assumed previously. The energy is evacuated by the radial expansion of the corona, leading to supersonic speeds of the solar wind. Magnetohydrodynamic (MHD) models assume collision-dominated solar wind and are also able to reproduce many solar wind characteristics. Nevertheless, the hypothesis of plasma dominated by collisions is not valid above the exobase. This highlights the complementarity of the MHD approach at low distances and the kinetic exospheric approach at larger distances, which can be combined for optimal solar wind results [37].

It is important to note that the effect of the electric field E is included in MHD hydrodynamic models as well [38]. Indeed, in the famous Parker model for instance [12], the hydrodynamic equations for electrons (index e) and protons

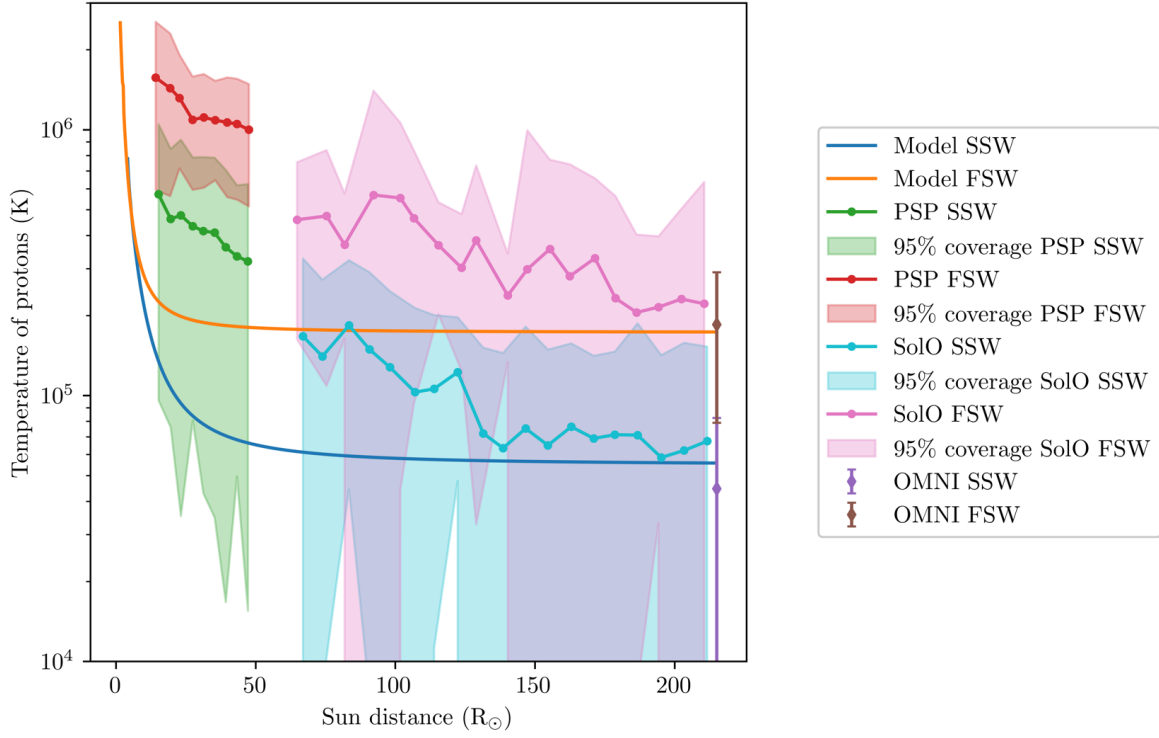


FIGURE 4. Averaged proton temperature as a function of the solar distance for the exospheric model constrained by averaged observations of Parker Solar Probe ($< 50 R_s$), Solar Orbiter ($> 63 R_s$), and OMNI ($215 R_s$) for fast solar wind (FSW in orange) and slow solar wind (SSW in blue).

(index p) are:

$$n_e m_e u_e \frac{\partial u_e}{\partial r} + \frac{\partial p_e}{\partial r} = -n_e m_e g - n_e e E \quad (1)$$

$$n_p m_p u_p \frac{\partial u_p}{\partial r} + \frac{\partial p_p}{\partial r} = -n_p m_p g + n_p e E \quad (2)$$

where p is the pressure, m the mass of the particle, g the gravitational acceleration, and e the electric charge.

By considering the following hypotheses:

- Quasi-neutrality: $n_e = n_p$
- No electric current: $u_p = u_e$

the global equation is then written by adding equations (1) and (2):

$$\rho u \frac{\partial u}{\partial r} + \frac{\partial p}{\partial r} = -\rho g \quad (3)$$

where ρ is the mass density.

The electric field has thus disappeared from the global equation of the solar wind plasma, but this does not mean that the electric field is null. More specifically, it is here ensuring the equality of the proton and electron fluxes so that there is no net current, just like in kinetic models.

One of the advantages of the kinetic exospheric approach is its ability to clearly emphasize that the acceleration of the solar wind is due to the electric force, reducing the gravitational attraction of the protons and heavy ions [7]. It is

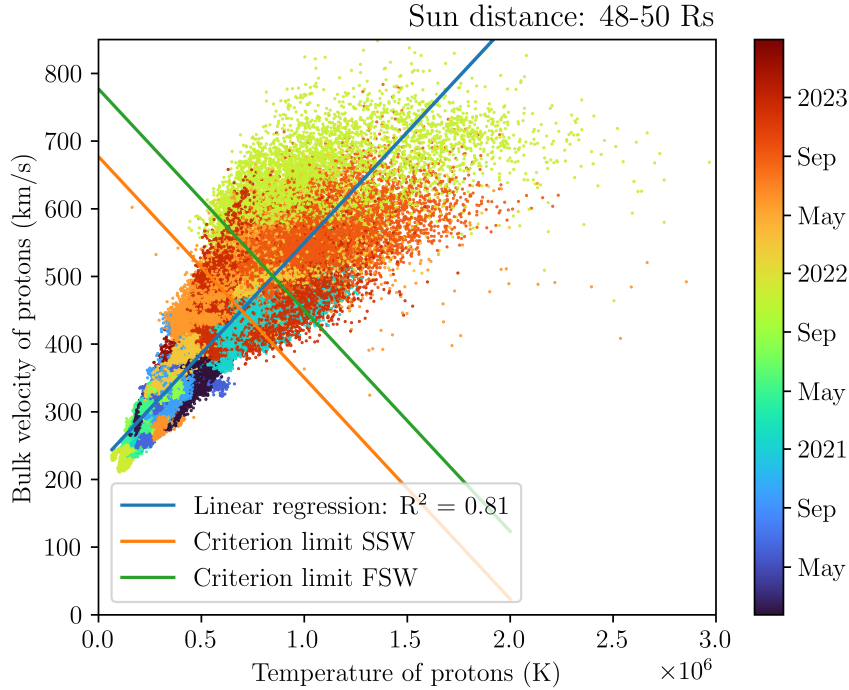


FIGURE 5. Proton bulk velocity as a function of the temperature of Parker Solar Probe observations between 48–50 R_s for all orbits from end of January 2020 to end of March 2023, excluding Solar Energetic Particle events. The linear regression considering the entire displayed data is shown in blue. The perpendicular orange and green lines respectively delimit the slow and fast winds (see text).

important to highlight that in the kinetic exospheric approach, the electric field is much higher than the Pannekoek-Rosseland [39] electric field, because of the presence of escaping particles [40]. Moreover, it allows to take into account suprathermal electrons using Kappa distributions [41].

Figure 6 illustrates the electric potential profiles found for the SSW and FSW with the Kappa exospheric model with the parameters of Table 1. To be accelerated to higher bulk velocities, the fast wind needs a higher potential difference between the exobase and the large radial distances. This is obtained by considering a lower exobase or by decreasing the kappa index. Halekas et al. (2022) [33] measured that the electric potential is higher in the slow wind than in the fast wind above 14 R_s . This is indeed obtained also in the model, as illustrated in Figure 6, due to the low exobase for the fast wind and a sufficiently higher exobase for the slow wind. The difference is rather slight in Figure 6 but can be increased considering a higher exobase for the slow wind, which does not considerably modify the SSW profile.

As illustrated in Figure 7, the heat flux obtained with the model decreases with the radial distance, as observed with PSP [42]. It is higher in the fast wind than in the slow wind. The heat flux produced by the model is too high in comparison to observations [19, 43]. This is expected since exospheric models give a maximum level of the possible heat flux. In fact, neither purely collisionless models nor purely collisional mechanisms are able to explain the heat flux decay as measured in the solar wind [44]. Whistler waves, commonly observed in the interplanetary space, are a good candidate to solve the problem of heat flux regulation [10]. Effects of whistler wave turbulence on the evolution of the electron distribution function in the solar wind were shown to be able to modify the suprathermal populations [9], and especially spread the strahl to the halo as observed in the solar wind [45]. Other plasma instabilities can also help to understand the characteristics of the observed distributions, and especially their temperature anisotropies and heat fluxes [46, 47].

For proton distributions, kinetic Alfvén wave turbulence presents another potential mechanism in the still-debated energy responsible for accelerating plasma and for the formation of the proton beam [48, 49]

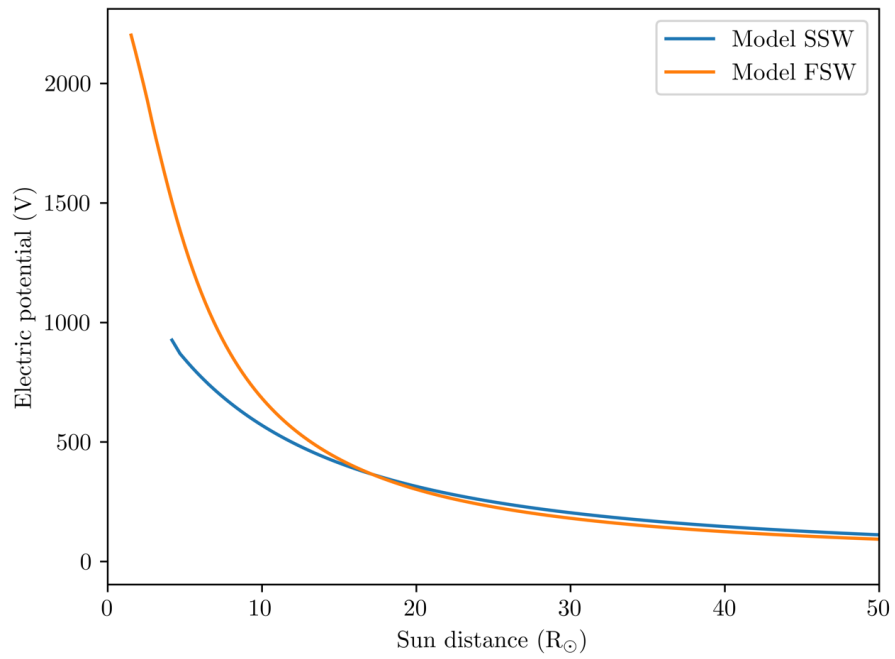


FIGURE 6. Electric potential obtained with the exospheric model using the parameters of Table 1 for the fast (orange) and slow wind (blue).

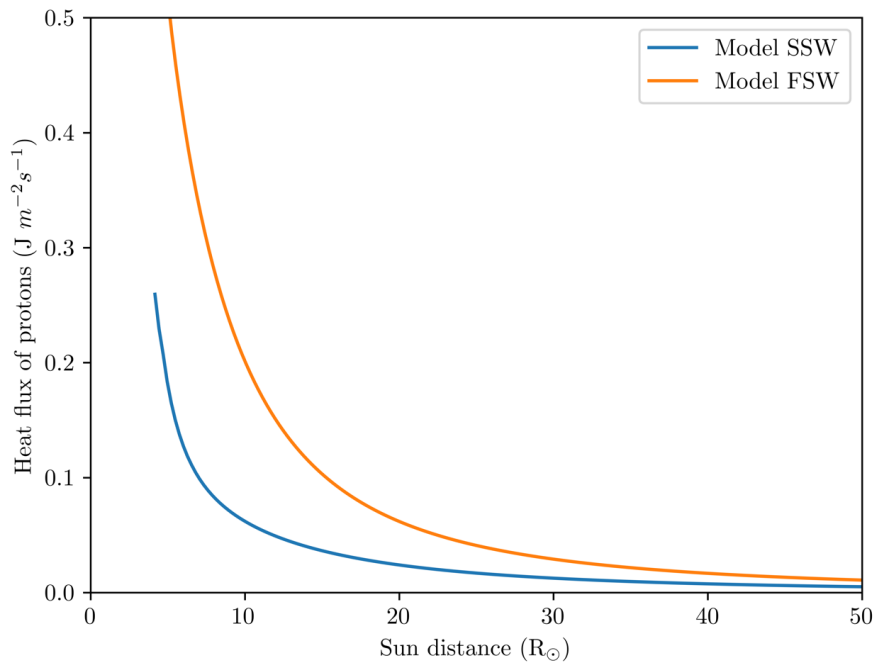


FIGURE 7. Heat flux obtained with the exospheric model using the parameters of Table 1 for the fast (orange) and slow wind (blue).

CONCLUSION

In this section, we summarize the main results of the present study.

- More precise boundary conditions were found for the exospheric model by constraining it with PSP, SoHO and OMNI observations from their launch to mid-2023. The values of the radial distance of the exobase, density, temperature and kappa index at the exobase for the slow and fast wind were determined to best fit the averaged profiles of the moments.
- The criterion distinguishing fast and slow wind was improved in the case of a significant remaining acceleration. This improvement shows that the acceleration of the solar wind seems to closely follow what was predicted by the exospheric model. This was achieved only by deducing the criteria from the observed correlation between wind speed and proton temperature.
- The exobase altitude also has important implications in the acceleration of the solar wind. This implies that the electric field can still be higher for slower winds if the exobase is substantially higher than for faster winds.
- It has been shown that the electric field is important also in MHD models.
- One of the main advantages of kinetic models is their ability to consider suprathermal particles.
- The exospheric models give a maximum heat flux, which can be improved by considering interactions between the particles. Fokker-Planck models including Coulomb collisions and wave-particle turbulence provide significant improvement concerning the regulation of the heat flux and the temperature anisotropy.

ACKNOWLEDGMENTS

The project 21GRD02 BIOSPHERE has received funding from the European Partnership on Metrology, co-financed by the European Union's Horizon Europe Research and Innovation Programme and by the Participating States.

REFERENCES

1. N. Meyer-Vernet, *Basics of the Solar Wind*, Cambridge Atmospheric and Space Science Series (Cambridge University Press, 2007).
2. A. Rouillard, N. Viall, C. Vocks, Y. Wu, R. Pinto, M. Lavarra, L. Matteini, V. Pierrard, and et al., "The solar wind," in *Solar Physics and Solar wind* (AGU Monograph, 2021).
3. V. Pierrard, "Kinetic models for solar wind electrons, protons and ions," in *Exploring the Solar Wind*, edited by M. Lazar (IntechOpen, Rijeka, 2012) pp. 221–240.
4. V. Pierrard and J. Lemaire, "Lorentzian ion exosphere model," *Journal of Geophysical Research* **103**, 7923–7934 (1996).
5. H. Lamy, V. Pierrard, M. Maksimovic, and J. Lemaire, "A kinetic exospheric model of the solar wind with a non monotonic potential energy for the protons," *J. Geophys. Res.* **108**, 1047–1057 (2003).
6. V. Pierrard and M. Lazar, "Kappa Distributions: Theory and Applications in Space Plasmas," *Sol. Phys.* **267**, 153–174 (2010).
7. V. Pierrard and H. Lamy, "The effects of the velocity filtration mechanism on the minor ions of the corona," *Sol. Phys.* **216**, 47–58 (2003).
8. V. Pierrard, M. Maksimovic, and J. Lemaire, "Self-consistent model of solar wind electrons," *Journal of Geophysical Research* **106**, 29,305–29,312 (2001b).
9. V. Pierrard, M. Lazar, and R. Schlickeiser, "Evolution of the electron distribution function in the wave turbulence of the solar wind," *Sol. Phys.* **269**, 421–438 (2011).
10. L. Colombari, *Interactions between whistler waves and solar wind suprathermal electrons: Solar Orbiter and Parker Solar Probe observations*, Ph.D. thesis, Université d'Orléans (2023).
11. J. Zhao, L. Lee, H. Xie, Y. Yao, D. Wu, Y. Voitenko, and V. Pierrard, "Quantifying Wave-particle Interactions in Collisionless Plasmas: Theory and Its Application to the Alfvén-mode wave," *The Astrophysical Journal* **930:95**, 28p (2022).
12. E. Parker, "Dynamics of the interplanetary gas and magnetic fields," *The Astrophysical Journal Letters* **128**, 664 (1958).
13. V. Pierrard, M. Lazar, S. Poedts, Š. Štverák, M. Maksimovic, and P. Trávníček, "The electron temperature and anisotropy in the solar wind. comparison of the core and halo populations," *Sol. Phys.* **291**, 2165–2179 (2016).
14. J. Zhao, M. D. Malaspina, T. Dudok De Wit, V. Pierrard, Y. Voitenko, G. Lapenta, S. Poedts, S. D. Bale, J. C. Kasper, D. Larson, R. Livi, and P. Whittlesey, "Broadband Electrostatic Waves in the Near-Sun Solar Wind Observed by the Parker Solar Probe," *The Astrophysical Journal Letters* **938(2)**, L21 (2022).
15. L. Berčič, D. Verscharen, C. J. Owen, L. Colombari, M. Kretzschmar, T. Chust, M. Maksimovic, D. O. Kataria, C. Anekallu, E. Behar, M. Berthomier, R. Bruno, V. Fortunato, C. W. Kelly, Y. V. Khotyaintsev, G. R. Lewis, S. Livi, P. Louarn, G. Mele, G. Nicolaou, G. Watson, and R. T. Wicks, "Whistler instability driven by the sunward electron deficit in the solar wind," *Astronomy and Astrophysics* **656**, 10 (2021).

16. J. S. Halekas, P. Whittlesey, D. Larson, M. Maksimovic, R. Livi, M. Berthomier, J. Kasper, A. Case, M. Stevens, S. Bale, and et al., “The Radial Evolution of the Solar Wind as Organized by Electron Distribution Parameters,” *The Astrophysical Journal* **936**, 10 p. (2022).
17. M. Maksimovic, A. Walsh, V. Pierrard, S. Štverák, and I. Zouganelis, “Electron Kappa distributions in the solar wind: cause of the acceleration or consequence of the expansion?” in *Kappa Distributions, From Observational Evidences via Controversial Predictions to a Consistent Theory of Nonequilibrium Plasmas* (Springer/Nature, 2021).
18. V. Pierrard, M. Maksimovic, and J. Lemaire, “Core, Halo and Strahl Electrons in the Solar Wind,” *Astrophys. Space Sci.* **277**, 195–200 (2001a).
19. V. Pierrard, M. Péters de Bonhome, J. Halekas, C. Audoor, P. Whittlesey, and R. Livi, “Exospheric solar wind model based on regularized kappa distributions for the electrons constrained by parker solar probe observations,” *Plasma* **6**, 518–540 <https://doi.org/10.3390/plasma6030036> (2023).
20. M. Maksimovic, V. Pierrard, and J. Lemaire, “A kinetic model of the solar wind with Kappa distributions in the corona,” *A&A* **324**, 725–734 (1997).
21. V. Pierrard and M. Pieters, “Coronal heating and solar wind acceleration for electrons, protons and minor ions obtained from kinetic models based on Kappa distributions,” *Journal of Geophysical Research* **119**, 9441–9455 (2014).
22. K. Scherer, H. Fichtner, and M. Lazar, “Regularized κ -distributions with non-diverging moments,” *EPL (Europhysics Letters)* **120**, 50002 (2017).
23. M. Lazar, K. Scherer, H. Fichtner, and V. Pierrard, “Toward a realistic macroscopic parametrization of space plasmas with regularized κ -distributions,” *A&A* **634**, A20 (2020).
24. V. Pierrard, M. Lazar, and M. Maksimovic, “Suprathermal populations and their effects in space plasmas: Kappa vs. Maxwellian,” in *Kappa Distributions, From Observational Evidences via Controversial Predictions to a Consistent Theory of Nonequilibrium Plasmas* (Springer/Nature, 2021).
25. M. Maksimovic, I. Zouganelis, J.-Y. Chaufray, K. Issautier, E. E. Scime, J. E. Littleton, E. Marsch, D. J. McComas, C. Salem, R. P. Lin, and H. Elliott, “Radial evolution of the electron distribution functions in the fast solar wind between 0.3 and 1.5 au,” *Journal of Geophysical Research* **110**, A09104 (2005), [10.1029/2005JA011119](https://doi.org/10.1029/2005JA011119).
26. J. D. Scudder, “Why all stars should possess circumstellar temperature inversions,” *The Astrophysical Journal* **398**, 319–349 (1992).
27. V. Pierrard, H. Lamy, and J. Lemaire, “Exospheric distributions of minor ions in the solar wind,” *J. Geophys. Res.* **109**, A02118 1–13 (2004).
28. J. Abraham, C. Owen, D. Verscharen, M. Bakrania, D. Stansby, R. Wicks, G. Nicolaou, P. Whittlesey, and et al., “Radial Evolution of Thermal and Suprathermal Electron Populations in the Slow Solar Wind from 0.13 to 0.5 au: Parker Solar Probe Observations,” *The Astrophysical Journal* **931**, 118 (2023).
29. V. Pierrard, M. Lazar, and S. Štverák, “Implications of the Kappa Suprathermal Halo of the Solar Wind Electrons,” *Frontiers in Astronomy and Space Sciences* **9** (2022), [10.3389/fspas.2022.892236](https://doi.org/10.3389/fspas.2022.892236).
30. M. Maksimovic, V. Pierrard, and P. Riley, “Ulysses electron distributions fitted with kappa functions,” *Geophysical Research Letters* **24**, 1151–1154 (1997).
31. V. Pierrard and N. Meyer-Vernet, “Electron Distributions in Space Plasmas,” in *Kappa Distributions: Theory and Applications in Plasmas*, edited by G. Livadiotis (Elsevier, 2017) pp. 465–479.
32. V. Pierrard, M. Lazar, and S. Štverák, “Solar wind plasma particles organized by the flow speed,” *Sol. Phys.* **295**, 151 1–14 (2020).
33. J. S. Halekas, L. Berčič, P. Whittlesey, D. Larson, R. Livi, M. Berthomier, J. Kasper, A. Case, M. Stevens, S. Bale, and et al., “The Sunward Electron Deficit: A Telltale Sign of the Sun’s Electric Potential,” *The Astrophysical Journal* **916** (2021), [10.3847/1538-4357/ac096e](https://doi.org/10.3847/1538-4357/ac096e).
34. M. Péters de Bonhome, *Analysis of the new solar wind observations for space weather modeling*, Master thesis, Université Catholique de Louvain (2023).
35. R. Livi and et al., “The Solar Probe Analyzer–Ions on the Parker Solar Probe,” *Astrophys. J.* **938**, 138 (2022).
36. M. Maksimovic, S. D. Bale, L. Berčič, J. W. Bonnell, A. W. Case, T. D. d. Wit, K. Goetz, J. S. Halekas, P. R. Harvey, K. Issautier, J. C. Kasper, K. E. Korreck, V. K. Jagarlamudi, N. Lahmiti, D. E. Larson, A. Lecacheux, R. Livi, R. J. MacDowall, D. M. Malaspina, M. M. Martinović, N. Meyer-Vernet, M. Moncuquet, M. Pulupa, C. Salem, M. L. Stevens, Š. Štverák, M. Velli, and P. L. Whittlesey, “Anticorrelation between the Bulk Speed and the Electron Temperature in the Pristine Solar Wind: First Results from the Parker Solar Probe and Comparison with Helios,” *The Astrophysical Journal Supplement Series* **246**, 62 (2020).
37. S. P. Moschou, V. Pierrard, R. Keppens, and J. Pomoell, “Interfacing MHD and kinetic solar Wind Models and comparing their energetics,” *Sol. Phys.* **292**, 1–9455 (2017).
38. V. Pierrard, *L’environnement spatial de la Terre* (Presses Universitaires de Louvain, Louvain-La-Neuve, 2009).
39. A. Pannekoek, “Ionization in stellar atmospheres,” *Bulletin Astron. Inst. Math.* **1**, 107–118 (1922).
40. J. Lemaire and V. Pierrard, “Kinetic models of solar and polar winds,” *Astrophys. Space Sci.* **277**, 169–180 (2001).
41. V. Pierrard, “Effects of suprathermal particles in space plasmas,” *ICNS Annual International Astrophysics Conf. Proc.* **1436**, 61–66 (2012).
42. J. S. Halekas, P. Whittlesey, D. E. Larson, D. McGinnis, M. Maksimovic, M. Berthomier, J. C. Kasper, A. W. Case, K. E. Korreck, M. L. Stevens, K. G. Klein, S. D. Bale, R. J. MacDowall, M. P. Pulupa, D. M. Malaspina, K. Goetz, and P. R. Harvey, “Electrons in the Young Solar Wind: First Results from the Parker Solar Probe,” *The Astrophysical Journal Supplement Series* **246**, 22 (2020).
43. V. Pierrard, “Solar wind electron transport: interplanetary electric field and heat conduction,” *Space Science Review* **172**, 315–324 (2012).
44. S. Bale and et al., “Electron heat conduction in the solar wind: transition from Spitzer-Harm to the collisionless limit,” *The Astrophysical Journal* **769**:2, 2041–8213 (2013).
45. S. Štverák, M. Maksimovic, P. Travníček, E. Marsch, A. Fazakerley, and E. Scime, “Radial evolution of nonthermal electron populations in the low-latitude solar wind: Helios, cluster, and ulysses observations,” *J. Geophys. Res.* **114**, 1–15 (2009).
46. H. Sun, J. Zhao, W. Liu, Y. Voitenko, V. Pierrard, C. Shi, Y. Yao, H. Xie, and D. Wu, “Electron heat flux instabilities in the inner heliosphere: Radial distribution and implication on the evolution of electron velocity distribution function,” *Astrophysical Journal Letters* **916**(1), L4 (2021).
47. D. Verscharen, B. D. G. Chandran, E. Boella, J. Halekas, M. E. Innocenti, V. Jagarlamudi, A. Micera, V. Pierrard, I. Vasko, and M. Velli, “Electron-driven instabilities in the solar wind,” *Frontiers in Astronomy and Space Sciences* **9** (2022), [10.3389/fspas.2022.951628](https://doi.org/10.3389/fspas.2022.951628).
48. V. Pierrard and Y. Voitenko, “Modification of the proton velocity distributions by Alfvénic turbulence in the solar wind,” *Solar Phys.* **288**, 355–368 (2013).
49. Y. Voitenko and V. Pierrard, “Proton beams generation by non-uniform solar wind turbulence,” *Solar Phys.* **290**, 1231–1241 (2015).